Tetrahedron: *Asymmetry* 24 (2013) 480–491

Contents lists available at SciVerse ScienceDirect

Tetrahedron: *Asymmetry*

journal homepage: www.elsevier.com/locate/tetasy

Synthesis of macrocycles and their application as chiral solvating agents in the enantiomeric recognition of carboxylic acids and α-amino acid derivatives

Shengnan Guo [a], Guo Wang [b], Lin Ai [a,*]

[a] College of Chemistry, Beijing Normal University, Beijing 100875, China
[b] Department of Chemistry, Capital Normal University, Beijing 100048, China

ARTICLE INFO

Article history:
Received 29 January 2013
Accepted 3 March 2013

ABSTRACT

The chiral macrocycles **1** and **2** with multiple binding sites have been synthesized from *D*-phenylalanine as chiral solvating agents (CSAs) for the enantiomeric discrimination and determination of the enantiomeric excess of carboxylic acids and a-amino acids derivatives by the ^{1}H NMR spectroscopy. The results show that chiral macrocycles **1** and **2** are effective CSAs towards the carboxylic acids and a-amino acids derivatives.

1. Introduction

Chiral recognition has received considerable attention in recent years due to the significant importance of chirality in biology, pharmaceutical chemistry, and asymmetric catalysis.[1] In the field of chirality and related research, the discrimination of the absolute configuration and the determination of the enantiomeric purity are indispensable to a chiral compound.[2] Therefore, many methods and techniques, such as HPLC,[3] NMR,[4] UV–vis,[5] and fluorescence spectroscopy,[6] have been developed and used to meet the increased demands of enantiomeric discrimination and analysis of enantiomeric excess. Among them, the NMR method has very distinct advantages, such as only requiring very little of the sample and deuterated solvent, less environmental pollution, and also being highly accurate, reliable, and convenient procedures.[1d–f,7] Thus, many types of chiral shift reagents (CSRs) and chiral solvating agents (CSAs), such as lanthanide complexes,[8] cyclodextrins,[9] crown ethers,[10] porphyrins,[11] calixarenes,[12] and others,[13] have been designed, synthesized, and screened for these purposes. To the best of our knowledge, these are the only receptors with a structure capable of differentiating the NMR signals of enantiomers upon complexation as CSRs or CSAs by NMR spectroscopy.[14] Recently, chiral macrocycles have been recognized as one of the most effective chiral solvating agents for chiral recognition by NMR spectroscopy due to their inherent reduced flexibility and complexation ability.[15] Herein we report the synthesis of novel chiral macrocycles **1** and **2** with multiple bonding sites from D-phenylalanine and their application in chiral recognition as chiral solvating agents toward carboxylic acids and α-amino acid derivatives by ^{1}H NMR spectroscopy.

2. Results and discussion

The chiral macrocycles **1** and **2** were designed and synthesized starting from D-phenylalanine. Their structures are shown in Figure 1.

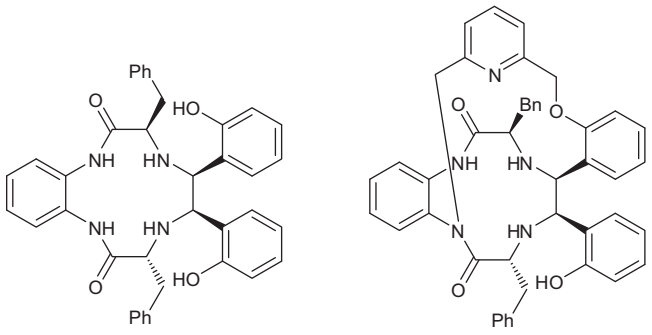

Figure 1. Structures of the chiral macrocycles **1** and **2**.

The *N*-Boc-protected D-phenylalanine **4** was obtained from D-phenylalanine **3** according to the literature.[16] The coupling reaction with **4** and *o*-phenylenediamine was carried out in the presence of *N*,*N*′-dicyclohexylcarbodiimide (DCC) in an ice-salt bath under a nitrogen atmosphere according to a modified procedure.[17] The crude product was purified by column chromatography on silica gel to afford the pure compound **5** in 83% yield. The chiral diamine **6** was prepared by deprotection of *N*-Boc-protected diamide **5** in trifluoroacetic acid (TFA) in 86% yield[17] (Scheme 1).

Chiral diimine **7** was obtained via condensation reaction of chiral diamine **6** with salicylaldehyde in 90% yield.[17] The reductive

* Corresponding author. Tel.: +86 1058807843.
E-mail address: linai@bnu.edu.cn (L. Ai).

0957-4166/$ - see front matter © 2013 Elsevier Ltd. All rights reserved.
http://dx.doi.org/10.1016/j.tetasy.2013.03.005

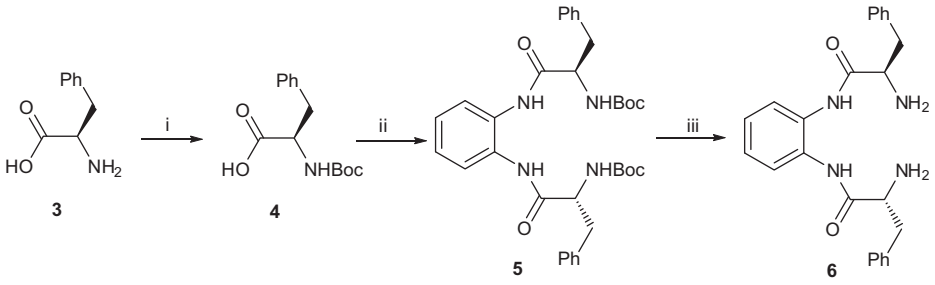

Scheme 1. Synthesis of chiral compounds **5** and **6**. Reagents and conditions: (i) NaOH (1 M), isopropanol, $(Boc)_2O$; (ii) EtOAc, *o*-phenylenediamine, ice-salt bath to rt, N_2; (iii) TFA, CH_2Cl_2, N_2.

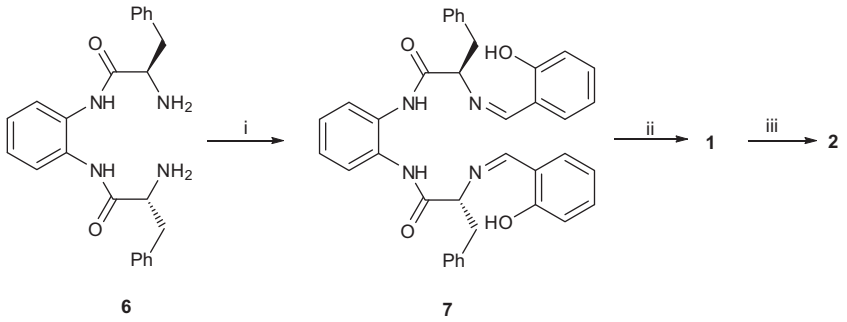

Scheme 2. Synthesis of chiral macrocycles **1** and **2**. Reagents and conditions: (i) CH_3OH, salicylaldehyde, reflux, N_2; (ii) DMF, Zn powder, MsOH, −35 °C to 0 °C; (iii) K_2CO_3, DMF, 2,6-dibromomethylpyridine, N_2.

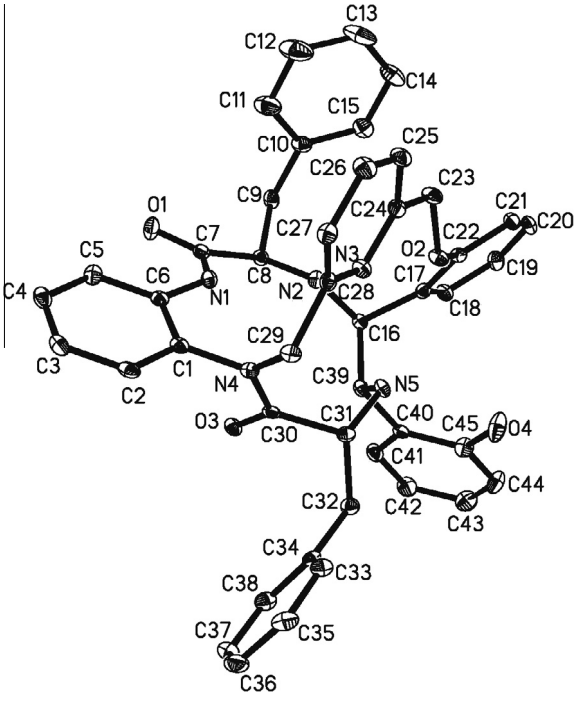

Figure 2. X-ray crystal structure of the chiral macrocycle **2**.

coupling reaction was performed for the preparation of chiral macrocycle **1** under the suitably dilute conditions.[18] However, despite our efforts, crystals suitable for X-ray crystal diffraction could not be obtained. The chiral macrocycle **2** was derived from macrocycle **1** with 2,6-dibromomethylpyridine in the presence of K_2CO_3 under a nitrogen atmosphere (Scheme 2).

Table 1
Measurements of ^1H chemical shift nonequivalence ($\Delta\Delta\delta$) of the guests (10×10^{-3} M) in the presence of CSAs **1**–**2** (10×10^{-3} M) by ^1H NMR spectroscopy (400 MHz) in $CDCl_3$ at 25 °C[a]

Entry	Guest	Proton	$\Delta\Delta\delta$ (Hz) (CSA **1**)	$\Delta\Delta\delta$ (Hz) (CSA **2**)
1	**8**	α-H	4.76	0.00
2	**9**	α-H	3.48	0.00
		OCH_3	15.16	0.00
3	**10**	$COCH_3$	25.36	3.24
		SCH_3	1.28	3.12
		α-H	24.04	0.00
4[b]	**11**	α-H	5.88	0.00
		CH_3	3.68	0.00
5[b]	**12**	α-H	2.92	0.00
6[b]	**13**	CH_3	3.96	2.24
7[b]	**14**	α-H	3.36	0.00
8	**15**	$COCH_3$	2.24	1.36
		OCH_3	1.76	0.00
9	**16**	PhCH_3	0.00	1.56
		SCH_3	8.16	14.20
10	**17**	CH_3	11.32	0.00
		PhCH_3	0.00	3.76
11	**18**	CH_3	36.16	16.20
		CH_3	25.44	6.28
		PhCH_3	8.32	2.12
12	**19**	CH_3	10.24	19.56
		CH_3	10.68	2.76
		PhCH_3	0.00	12.68
13[b]	**20**	α-H	24.68	0.00
		CH_3	6.20	0.00
14	**21**	CH_3	10.20	9.16
15	**22**	CH_3	2.92	0.00
16[b,c]	**23**	α-H	17.44	3.08
17[b]	**24**	α-H	5.20	0.00

[a] Typical conditions: concentration of the guest and the CSA **1** or **2** was 10 mM (1:1) in 0.5 mL of $CDCl_3$, and the spectra were recorded at 25 °C.
[b] Using $CDCl_3/CD_3OD$ (5%) as solvents.
[c] Concentration of the guest was 2.5 mM.

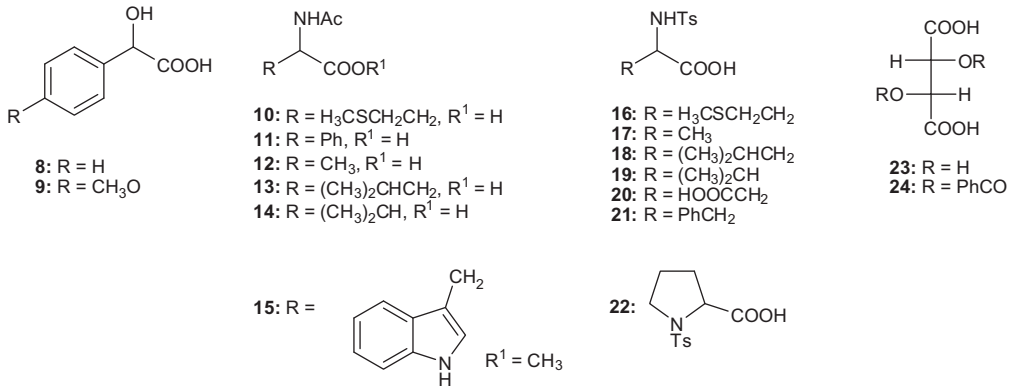

Figure 3. Structures of the carboxylic acids and α-amino acid derivatives.

The crystals of macrocycle **2** were grown by slow evaporation from a mixture of methanol and acetone for X-ray crystal diffraction.[19] The structure of chiral macrocycle **2** was confirmed as having an (*R*,*S*,*R*,*R*)-configuration by X-ray crystallography (Fig. 2).

The structure of chiral macrocycle **1** is shown to have an (*R*,*S*,*R*,*R*)-configuration and is a 12-membered ring product based on the X-ray structure of chiral macrocycle **2**. In addition, the structures of chiral macrocycles **1** and **2** were also characterized by ^{1}H NMR, ^{13}C NMR, HRMS, and IR.

In order to explore the binding properties of chiral macrocycles **1** and **2** as CSAs for carboxylic acids and α-amino acid derivatives by NMR spectroscopy, the following carboxylic acids and α-amino acid derivatives were chosen as guests (Fig. 3).

The ^{1}H NMR spectra of the carboxylic acids **8**–**9** and α-amino acid derivatives **10**–**24** were measured in the presence of the macrocycles **1** and **2** as chiral solvating agents, respectively. Macrocycle **1** exhibited stronger binding properties, a better baseline resolution, and a fairly wide detection window, for example, the maximum chemical shift nonequivalence of the CH*CH*$_3$ signals of **18** was 36.16 Hz (Table 1, entry 11). These results demonstrated that macrocycle **1** was a highly effective chiral solvating agent for carboxylic acids and α-amino acid derivatives. However, macrocycle **2** was only able to recognize some of the above carboxylic acids and α-amino acid derivatives under the same conditions. Detailed results are summarized in Table 1.

When mixing **21** and CSA **1** or **2** with a 1:1 molar ratio, the signals of the CH$_3$– protons of **21** were split into two equal-intensity peaks by ^{1}H NMR spectroscopy on a 400 MHz instrument. Compared to the chemical shift values (2.3982 ppm) of the CH$_3$– protons of free **21**, the chemical shift values of the CH$_3$– protons of (*R*)- and (*S*)-**21** exhibited an upfield shift of 0.0604 and 0.0859 ppm in the presence of CSA **1** and 0.0968 and 0.0739 ppm in the presence of CSA **2**, respectively. The chemical shift changes ($\Delta\delta_S$) of (*S*)-**21** were larger than those ($\Delta\delta_R$) of (*R*)-**21** in the presence of CSA **1**. In contrast, the chemical shift changes ($\Delta\delta_S$) of (*S*)-**21** were smaller than those ($\Delta\delta_R$) of (*R*)-**21** in the presence of CSA **2**. The chemical shift nonequivalence ($\Delta\Delta\delta$) of **21** was evaluated in 0.0255 and 0.0229 ppm in the presence of CSA **1** or **2**,

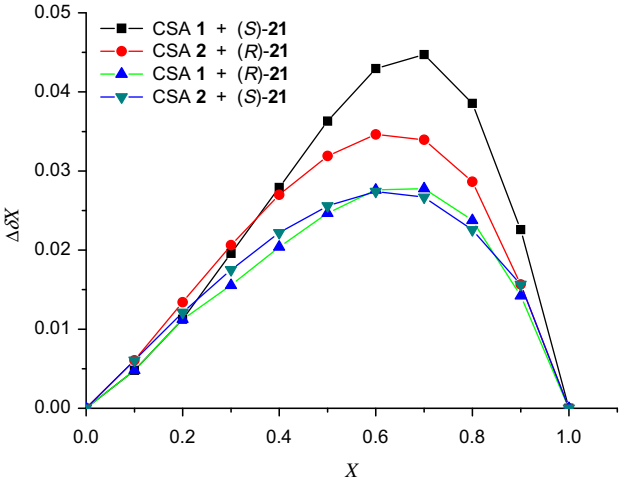

Figure 5. Job plots for the complexation of (*R*)- or (*S*)-**21** with CSA **1** and **2**. $\Delta\delta$ stands for chemical shift change of the CH$_3$-protons of (*R*)- or (*S*)-**21** in the presence of CSA **1** or **2**, *X* stands for the molar fraction of **21**, (*X* = [**21**]/([**21**] + [CSA **1** or **2**]).

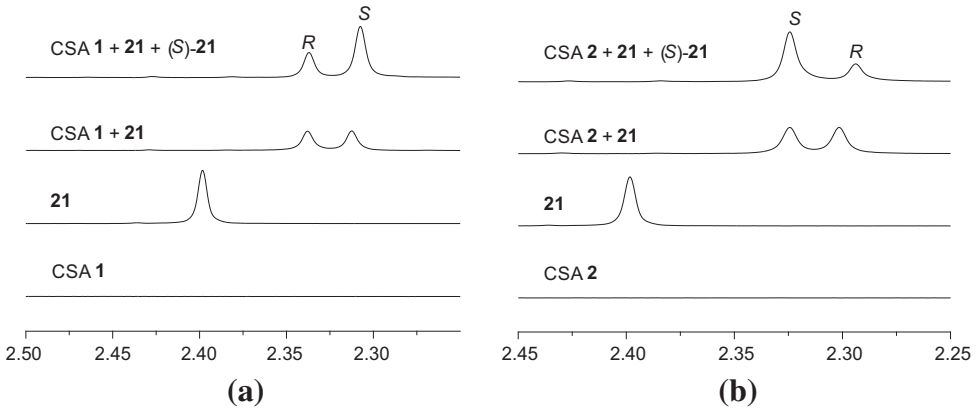

Figure 4. (a) The overlaid ^{1}H NMR spectra of free CSA **1**, free **21**, the 1:1 mixture of CSA **1** with **21**, the 1:2 mixture of (*R*)- and (*S*)-**21** in the presence of CSA **1**. (b) The overlaid ^{1}H NMR spectra of free CSA **2**, free **21**, and the 1:1 mixture of CSA **2** with **21**, the 1:2 mixture of (*R*)- and (*S*)-**21** in the presence of CSA **2**.

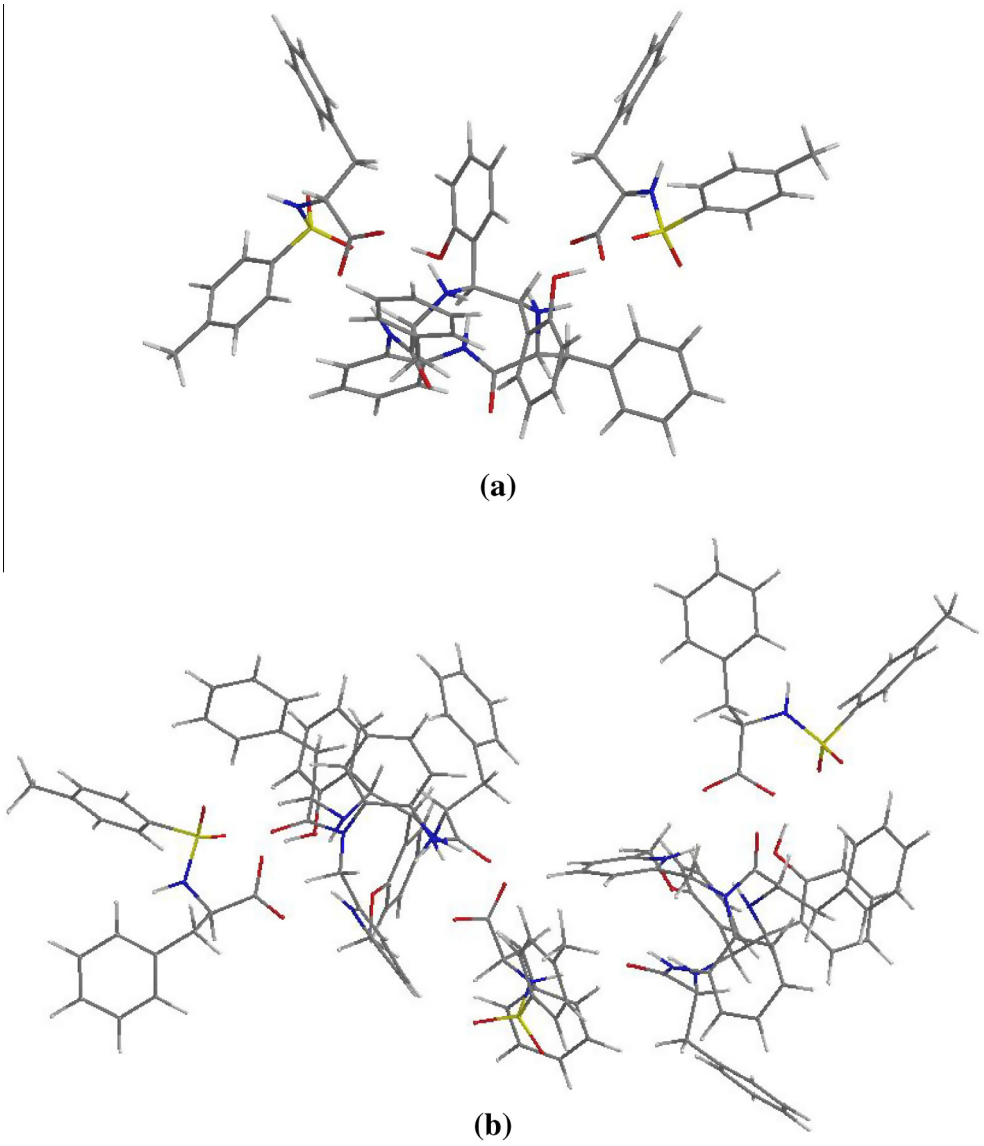

Figure 6. Proposed 1:2 and 2:3 binding models for the interactions of CSA **1** (a) and CSA **2** (b) with (*R*)-**21**, respectively.

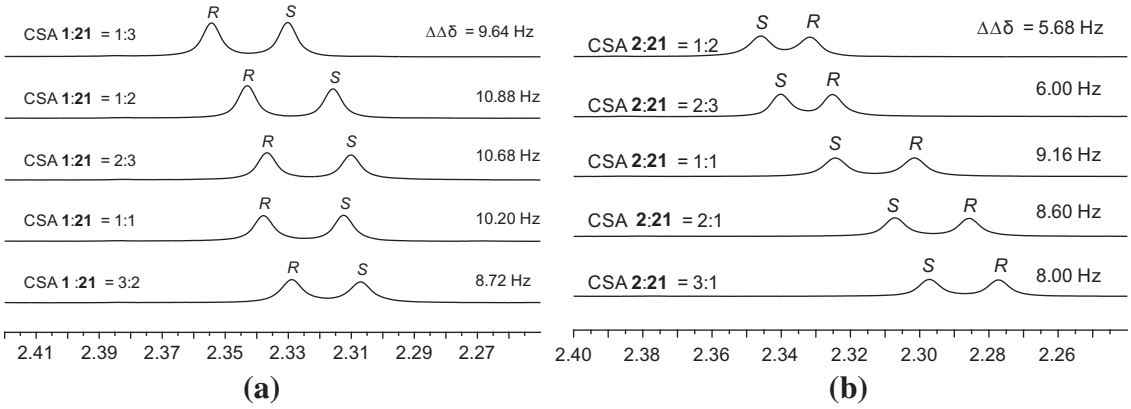

Figure 7. The overlaid ^{1}H NMR spectra of various molar ratio mixtures of CSA **1** with **21** (a) and CSA **2** with **21** (b). The concentration of **21** was 10 mM in $CDCl_3$.

respectively. Meanwhile, the enantiomeric discriminations of racemic **21** were determined by integration changes of the CH_3– protons of **21** by adding (*S*)-**21** to a 1:1 mixture of **21** and CSA **1** or CSA **2** in $CDCl_3$. The following spectra are presented with good baseline resolution and a fairly wide detection window, which show the potential of macrocycles **1** and **2** as CSAs for **21** (Fig. 4).

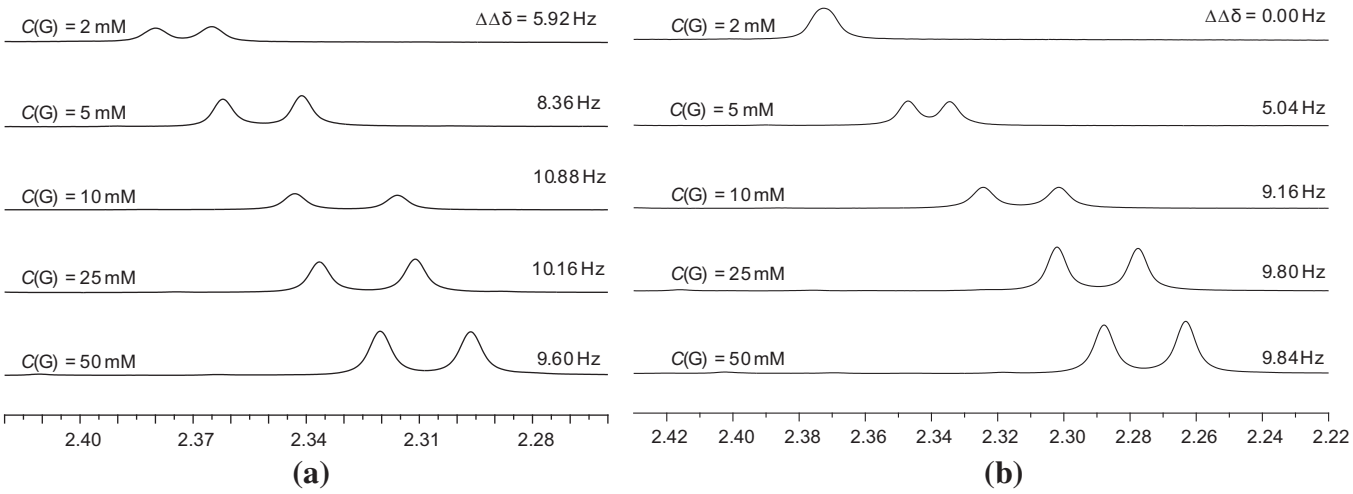

Figure 8. (a) Concentration variation of $\Delta\Delta\delta$ for **21** in the presence of CSA **1**. (b) Concentration variation of $\Delta\Delta\delta$ for **21** in the presence of CSA **2**. The molar ratio of CSA **1** or **2** versus **21** was 1:2 or 1:1, and was unchanged.

Table 2
Measurements of the ^{1}H chemical shift nonequivalence ($\Delta\Delta\delta$) of CH_3-protons of **21** in the presence of CSA **1** or CSA **2** by ^{1}H NMR spectroscopy (400 MHz) in different deuterated solvents[a]

Entry	Solvent	$\Delta\Delta\delta$ (Hz) (CSA **1**)[b]	$\Delta\Delta\delta$ (Hz) (CSA **2**)[c]
1	$CDCl_3$	10.88	9.16
2	$CDCl_3/C_6D_6$ (10%)	9.32	8.00
3	$CDCl_3/CD_3COCD_3$ (10%)	4.60	0.00
4	$CDCl_3/CD_3OD$ (10%)	0.00	0.00
5	$CDCl_3$/DMSO-d_6 (10%)	0.00	0.00

[a] All samples were prepared by mixing CSA **1** or CSA **2** with **21** (1:2; 1:1) in NMR tubes.
[b] The final concentrations of CSA **1** and **21** were 5 and 10 mM in 0.5 mL of various deuterated solvents.
[c] The final concentrations of CSA **2** and **21** were 10 mM in 0.5 mL of various deuterated solvents.

The Job plots of racemic **21** with CSA **1** or **2** were obtained with a total concentration of 10 mM. The maxima were observed at $X = 0.67$ and 0.60 until the molar ratios of CSA **1** or **2** versus **21** were 1:2 or 2:3, respectively. These indicate that 1 molecule of CSA **1** can bind with 2 molecules of **21** to form a complex or that 2 molecules of CSA **2** can bind with 3 molecules of **21** to form a complex. However, in theory, three kinds of complexes (*R*)/(*R*)-, (*R*)/(*S*)-, and (*S*)/(*S*)-**21** with CSA **1** should be generated based on the Job plots. Three sets of signals of the tosyl methyl group of **21** should also be observed in the ^{1}H NMR measurements. However, only two sets of ^{1}H NMR signals of the tosyl methyl group of (*R*)/(*R*)- and (*S*)/(*S*)-**21** were obtained in the presence of CSA **1**. These results may be due to a faster exchange over the NMR time-scale among the free guest, host, and their complexes. The Job plots of (*S*)- and (*R*)-**21** with CSA **1** or **2** are shown in Figure 5.

Theoretical calculations were performed using an AM1 model by using a GAUSSIAN 03 program[20] in order to investigate the interactions between CSA **1** or **2** with (*R*)-**21**. The proposed binding models for the interactions of CSA **1** and **2** with (*R*)-**21** are shown in Figure 6.

Upon the addition of CSA **1** or **2**, the nonequivalent chemical shifts of the CH_3-protons of (*R*)- and (*S*)-**21** were found to gradually increase until the molar ratios of CSA **1** and **2** to racemic **21** were 1:2 and 1:1, respectively. However, with the continued addition of CSA **1** or **2**, the nonequivalent chemical shifts showed a declining trend. The maximum nonequivalent chemical shifts ($\Delta\Delta\delta$) of **21** were obtained at 10.88 and 9.16 Hz in the presence of CSA **1** and **2**, respectively. Thus, the molar ratios of CSA **1**–**21** with 1:2 and CSA **2**–**21** with 1:1 were the best value for the enantiomeric discrimination of racemic **21** (Fig. 7).

In order to further study the binding properties, the ^{1}H NMR spectra of the various concentrations of **21** were performed in the presence of CSA **1** or **2**. With variation in concentration, a series of nonequivalent chemical shifts of **21** were observed from 5.92 to 9.60 Hz in the presence of CSA **1**. Among them, the concentration of 10 mM proved to be the best for the enantiomeric discrimination of **21** based on the maximum nonequivalent chemical shift at 10.88 Hz (Fig. 8a). However, when increasing the concentration, a slow increase of the nonequivalent chemical shifts of **21** was observed from 0.00 to 9.84 Hz in the presence of the CSA **2** and a maximum was not found (Fig. 8b). Based on the experimental results and the general requirements for concentration in ^{1}H NMR spectroscopy, a concentration of 10 mM was used for the enantiomeric discrimination of the carboxylic acids and α-amino acid derivatives in the presence of CSA **2**.

Additional ^{1}H NMR experiments of **21** were performed in order to study solvent effects in the presence of CSA **1** or **2** with a 1:2 or 1:1 molar ratio in $CDCl_3$ containing 10% different deuterated solvents. The experimental results are summarized in Table 2.

As shown in Table 2, upon the addition of the polar solvents, the binding interactions of **21** with CSA **1** or **2** were weakened and even removed. For example, the nonequivalent chemical shifts of **21** were changed from 10.88 Hz in $CDCl_3$ to 9.32 Hz in $CDCl_3$/benzene-d_6 (10%), 4.60 Hz in $CDCl_3$/acetone-d_6 (10%), and 0.00 Hz in $CDCl_3$/methanol-d_4 (10%) and $CDCl_3$/DMSO-d_6 (10%) in the presence of CSA **1**, respectively. Thus, solvents with less polarity were more suitable for studies on the chiral recognition by ^{1}H NMR spectroscopy, such as chloroform-*d* and benzene-d_6, if the solubility of guest and host was large enough for NMR testing.

To further explore the practical applications in both the discrimination of enantiomers and the determination of enantiomeric excess by NMR spectroscopy, the ^{1}H NMR spectra of the carboxylic acids and α-amino acid derivatives were measured by adding either the (*R*)- or (*S*)-enantiomer to a solution containing a racemic guest and CSA **1** or **2** with a 1:1 molar ratio. However in some cases, the enantiomeric discriminations of a few of the guests were determined by comparison to the chemical shift value of the corresponding (*R*)- or (*S*)-enantiomer in the presence of CSA **1** or **2** under the same conditions. A mixture of $CDCl_3$ with 5% CD_3OD was used due to the poor solubility of some carboxylic acids and α-amino acid derivatives in $CDCl_3$. The results are summarized in Table 3.

Table 3
Enantiomeric discrimination of the guests (10×10^{-3} M) and different concentrations of the (*S*)- or (*R*)-guest in the presence of CSA **1** or **2** (10×10^{-3} M) by ^{1}H NMR spectroscopy in $CDCl_3$ at 25 °C[a]

Entry	Guest	Proton	Spectrum (CSA **1**)	Spectrum (CSA **2**)
1	(±)-**8**	α-H	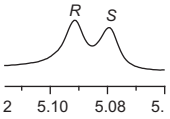	–
	(*S*)-**8**	α-H	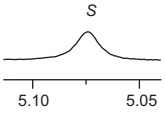	–
	(*R*)-**8**	α-H	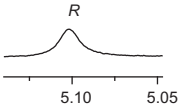	–
2	(±)-**9**	OCH_3	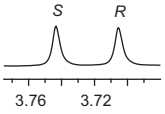	–
	(±)-**9**+(*S*)-**9**	OCH_3	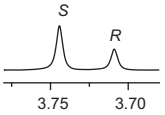	–
3	(±)-**10**	$COCH_3$	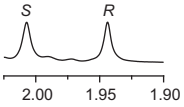	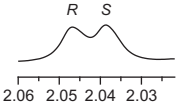
	(±)-**10**+(*S*)-**10**	$COCH_3$	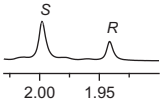	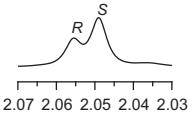
4[b]	(±)-**11**	α-H	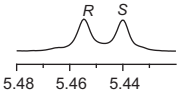	–
	(±)-**11**+(*S*)-**11**	α-H	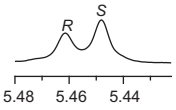	–
	(±)-**11**	CH_3	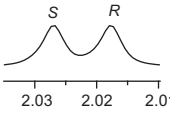	–
	(±)-**11**+(*S*)-**11**	CH_3	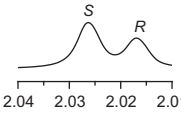	–
5[b]	(±)-**12**	α-H	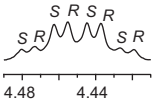	–
	(*S*)-**12**	α-H	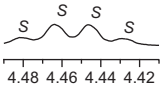	–
6[b]	(±)-**13**	CH_3	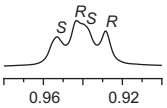	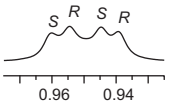
	(±)-**13**+(*S*)-**13**	CH_3	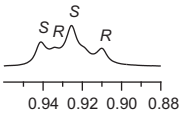	–

(*continued on next page*)

Table 3 (*continued*)

Entry	Guest	Proton	Spectrum (CSA **1**)	Spectrum (CSA **2**)
	(*S*)-**13**	CH_3	—	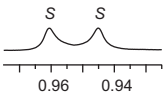
7[b]	(±)-**14**	α-H	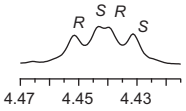	—
	(±)-**14**+(*S*)-**14**	α-H	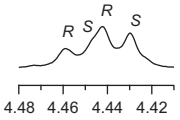	—
8	(±)-**15**	CH_3	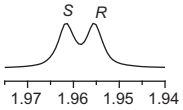	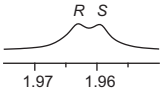
	(±)-**15**+(*S*)-**15**	CH_3	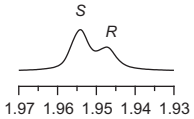	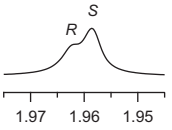
9	(±)-**16**	SCH_3	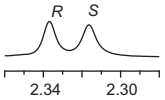	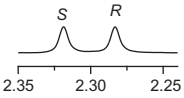
	(±)-**16**+(*S*)-**16**	SCH_3	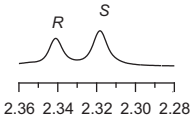	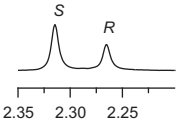
10	(±)-**17**	CH_3	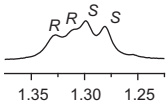	—
	(*S*)-**17**	CH_3	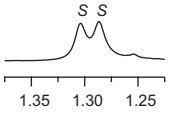	—
	(±)-**17**	$PhCH_3$	—	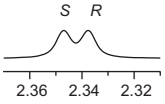
	(±)-**17**+(*S*)-**17**	$PhCH_3$	—	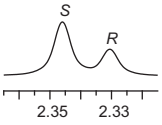
11	(±)-**18**	CH_3	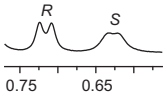	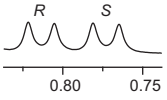
	(*S*)-**18**	CH_3	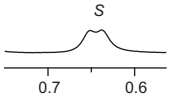	—
	(±)-**18**+(*S*)-**18**	CH_3	—	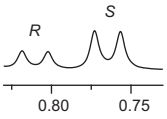
	(±)-**18**	CH_3	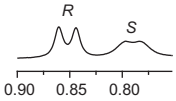	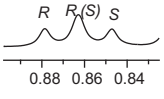

Table 3 (*continued*)

Entry	Guest	Proton	Spectrum (CSA **1**)	Spectrum (CSA **2**)
	(*S*)-**18**	CH_3	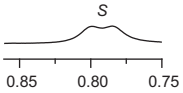	–
	(±)-**18**+(*S*)-**18**	CH_3	–	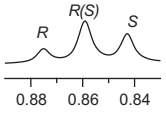
	(±)-**18**	$PhCH_3$	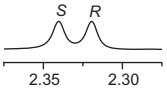	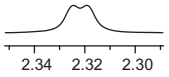
	(*S*)-**18**	$PhCH_3$	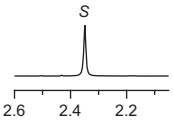	–
	(±)-**18**+(*S*)-**18**	$PhCH_3$	–	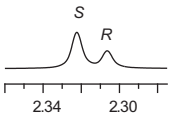
12	(±)-**19**	CH_3	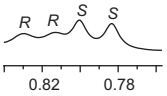	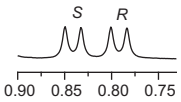
	(*S*)-**19**	CH_3	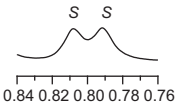	–
	(±)-**19**+(*S*)-**19**	CH_3	–	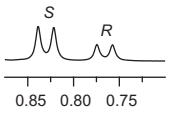
	(±)-**19**	$PhCH_3$	–	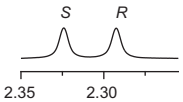
	(±)-**19**+(*S*)-**19**	$PhCH_3$	–	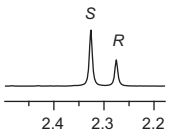
13[b]	(±)-**20**	α-H	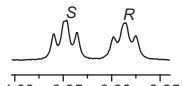	–
	(±)-**20**+(*S*)-**20**	α-H	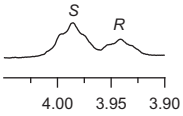	–
14	(±)-**21**	CH_3	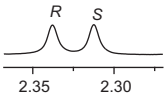	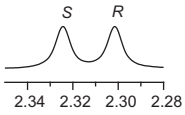
	(±)-**21**+(*S*)-**21**	CH_3	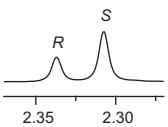	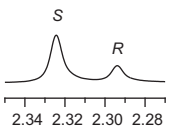
15	(±)-**22**	CH_3	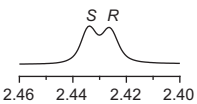	–

(*continued on next page*)

Table 3 (*continued*)

Entry	Guest	Proton	Spectrum (CSA **1**)	Spectrum (CSA **2**)
	(±)-**22**+(*S*)-**22**	CH_3	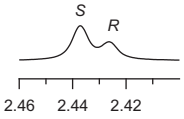	–
16[b,c]	(±)-**23**	α-H	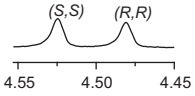	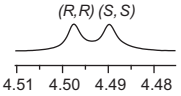
	(±)-**23**+(*R*,*R*)-**23**	α-H	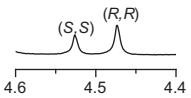	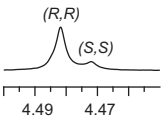
17	(±)-**24**	α-H	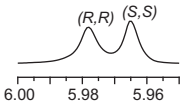	–
	(±)-**24**+(*R*,*R*)-**24**	α-H	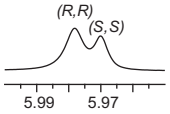	–

[a] Typical conditions: concentration of the guest and the CSA **1** or **2** is 10 mM (1:1) and various molar ratios of the (*S*)- or (*R*)-isomer in 0.5 mL of $CDCl_3$, and the spectra are recorded at 25 °C. The *R* and *S* in the spectra represent the signals of (*R*)- and (*S*)-isomers, respectively.
[b] Using $CDCl_3/CD_3OD$-d_4 (5%) as solvents.
[c] Concentration of the guest is 2.5 mM.

In order to evaluate the accuracy of the enantiomeric excess determined by ^{1}H NMR spectroscopy, all samples were prepared by mixing CSA **1** or **2** and **21** with 60%, 40%, 20%, 0%, −20%, −40%, and −60% ee according to 1:2 molar ratio of CSA **1** with **21** and a 1:1 molar ratio of CSA **2** with **21** in $CDCl_3$, respectively. The ^{1}H NMR spectra of **21** with different enantiomeric compositions were recorded in the presence of CSA **1** or CSA **2** by using the ^{1}H NMR method with a 400 MHz instrument. The enantiomeric excess of all samples was calculated based on the integration of the signals of the CH_3– protons of (*R*)- and (*S*)-**21** in the presence of CSA **1** or **2**. The results are shown in Figure 9.

The results indicate that the analysis of the enantiomeric excess has a high accuracy when using ^{1}H NMR spectroscopy in the presence of macrocycles **1** and **2** as CSAs ($y = 1.0087x - 0.5043$, correlation coefficient = 0.9998; $y = 1.0192x - 0.2184$, correlation coefficient = 0.9996). The linear correlation between the theoretical (y) and observed ee% values (x) is shown in Figure 10.

3. Conclusion

In conclusion, chiral macrocycles **1** and **2** have been synthesized starting from D-phenylalanine and have been proven to be effective chiral solvating agents for the enantiomeric discrimination and determination of the enantiomeric excess of carboxylic acids and α-amino acid derivatives by ^{1}H NMR spectroscopy.

4. Experimental

4.1. General

NMR spectra were recorded on a Bruker Advance II spectrometer at 400 MHz for ^{1}H NMR and 100 MHz for ^{13}C NMR. HRMS spectra were recorded on a LCT Premier XE spectrometer. IR spectra were obtained on a Nicolet 360 Avatar IR spectrometer as KBr pellets. Optical rotations were measured with a Perkin–Elmer Model 343 polarimeter using the sodium D line at 589 nm. X-ray crystal structure was determined by a Smart Apex II Single Crystal Diffractometer.

4.2. Synthesis of chiral macrocycle (*R*,*S*,*R*,*R*)-1

To a stirred suspension of diimine **7** (3.054 g, 5 mmol) and zinc powder (5.27 g, 50 mmol) in dry DMF (80 mL), a solution of MsOH (4.806 g, 50 mmol) in dry DMF (20 mL) was added dropwise over a period of 30 min at −35 °C under a nitrogen atmosphere. The mixture was stirred for 10 h at −35 °C to 0 °C. The reaction mixture was basified to pH 8–9 with saturated $NaHCO_3$. Next, $CHCl_3$ (50 mL) was added to the above mixture and then stirred for 1 h at room temperature. The organic phase was separated and the water phase was extracted with $CHC1_3$ (15 mL × 3). The combined organic phase was washed with distilled water (30 mL × 3), dried over anhydrous Na_2SO_4 overnight, and concentrated. The residue was purified by column chromatography on silica gel (petroleum/ethyl acetate = 2/1) to afford macrocycle **1** in 21.6% yield as a white solid. Mp 164–166 °C. R_f = 0.25 (petroleum/EtOAc = 2/1). $[\alpha]_D^{20} = -202.9$ (*c* 0.05, $CHC1_3$), ^{1}H NMR (400 MHz, $CDCl_3$) δ 2.75 (d, J = 10.9 Hz, 1H), 2.92–2.95 (m, 2H), 3.00–3.04 (m, 1H), 3.17 (d, J = 10.2 Hz, 1H), 3.59 (s, 2H), 4.27 (d, J = 9.4 Hz, 1H), 4.53 (s, 1H), 5.85 (d, J = 6.7 Hz, 2H), 6.30 (br, 1H), 6.49 (q, J = 7.3 Hz, 1H), 6.57 (d, J = 8.0 Hz, 1H), 6.72–6.81 (m, 5H), 6.92–6.98 (m, 6H), 7.05–7.10 (m, 5H), 7.88 (d, J = 7.7 Hz, 1H), 9.33 (br, 1H), 10.4 (br, 1H). ^{13}C NMR (100 MHz, $CDCl_3$) δ 34.5, 38.4, 62.0, 64.7, 66.5, 72.5, 116.1, 116.9, 119.1, 119.4, 120.5, 122.3, 124.3, 124.8, 126.5, 127.0, 127.8, 128.4, 128.6, 129.4, 131.1, 133.0, 136.2, 138.0, 154.5, 158.4, 171.8, 173.1. IR (KBr) 3284, 3051, 3029, 2924, 1665, 1594, 1532, 1455, 1257, 751, 700 cm^{-1}. HRMS(ES$^+$): calcd for $C_{38}H_{37}N_4O_4$ $(M+H)^+$ 613.2815, found 613.2802.

4.3. Synthesis of chiral macrocycle (*R*,*S*,*R*,*R*)-2

A mixture of macrocycle **1** (123 mg, 0.2 mmol) and 2,6-dibromethylpyridine (53 mg, 0.2 mmol) was stirred in the presence of K_2CO_3 (276 mg, 2 mmol) in dry DMF (4 mL) at room temperature

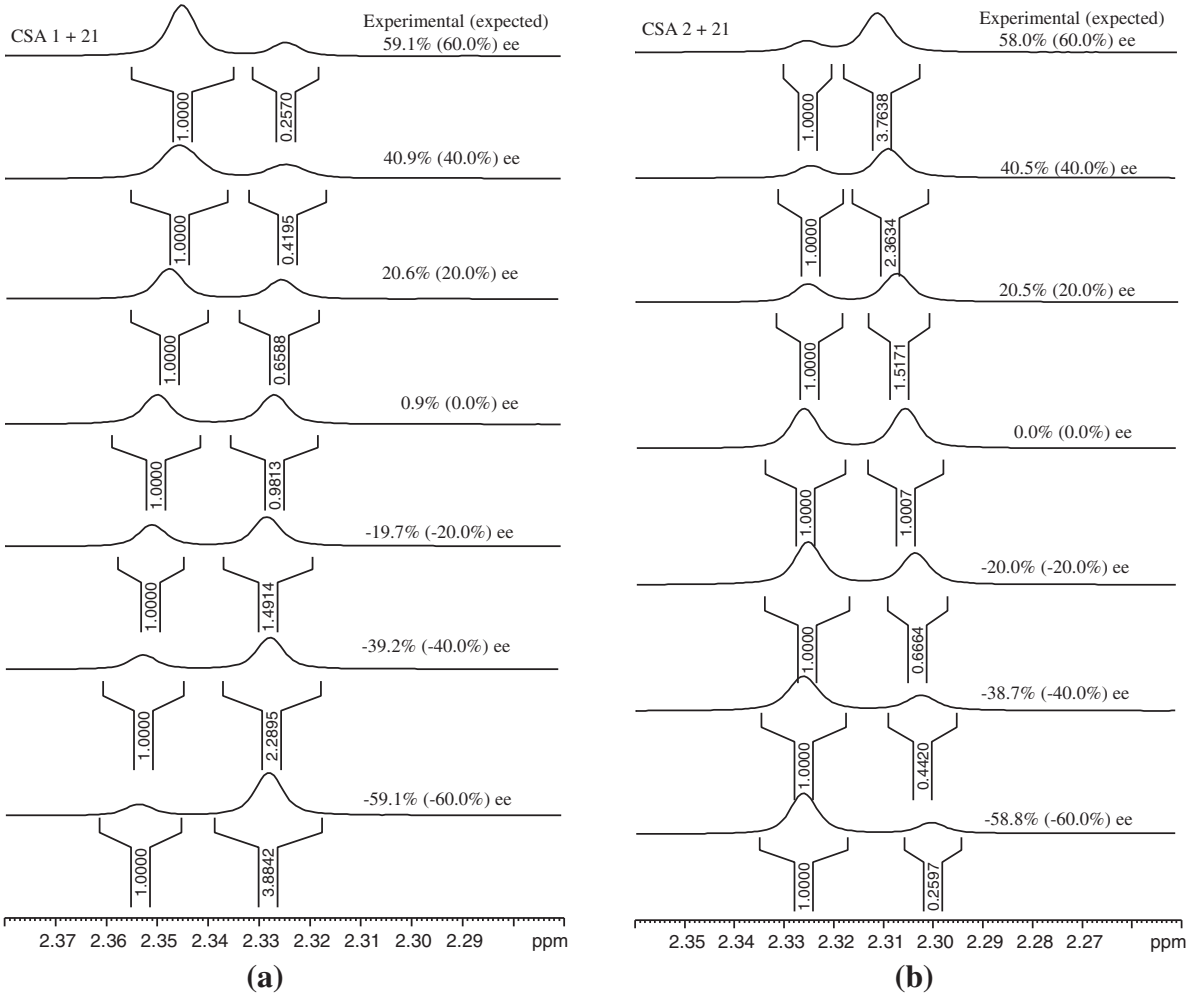

Figure 9. Determination of the enantiomeric purity of **21** (ee% = *R*–*S*%), the *R* and *S* stand for the protons from the CH_3 group of the corresponding (*R*)- and (*S*)-isomer of **21** in the presence of 0.5 equiv of CSA **1** (a); in the presence of 1.0 equiv of CSA **2** (b).

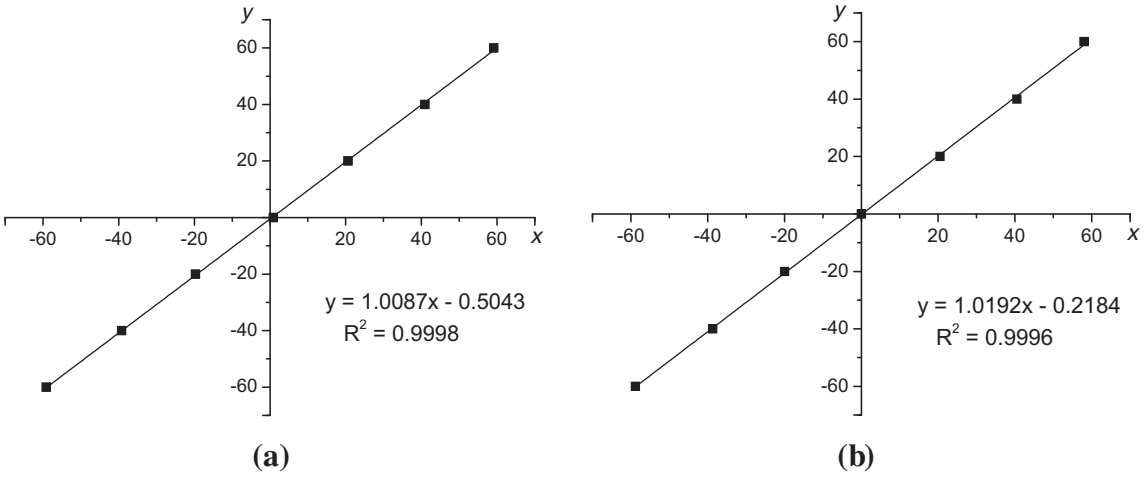

Figure 10. The linear correlation between the observed (*Y*) and theoretical ee% values (*X*) of **21** in the presence of 0.5 equiv of CSA **1** (a); in the presence of 1.0 equiv of CSA **2** (b).

for 10 h, after which water (20 mL) was added to quench the reaction. The mixture was extracted with $CHC1_3$ (5 mL × 3), and washed with water (20 mL × 2) and brine (20 mL). The organic layer was dried over Na_2SO_4 overnight and concentrated. The residue was purified by column chromatography on silica gel (petroleum/acetyl acetate/dichloromethane = 6/1/1.4) to afford macrocycle **2** as a

white solid in 54.3% yield. The crystals suitable for X-ray diffraction were obtained from methanol–acetone (5:2) as colorless crystals. 194–196 °C. R_f = 0.2 (petroleum/EtOAc = 2/1), $[\alpha]_D^{20} = -77.85$ (*c* 0.06, $CHC1_3$). ^{1}H NMR (400 MHz, DMSO-d_6) δ 2.67–2.73 (m, 2H), 3.05–3.14 (m, 3H), 3.56–3.57 (m, 1H), 3.59–3.64 (m, 1H), 4.36 (d, *J* = 16.1 Hz, 1H), 4.84–4.88 (m, 2H), 4.92 (d, *J* = 15.9 Hz, 1H), 5.03 (d, *J* = 4.2 Hz, 1H), 5.15 (d, *J* = 11.2 Hz, 1H), 5.85 (dd, *J* = 7.5 Hz, *J* = 1.4 Hz, 1H), 6.11 (d, *J* = 2.3 Hz, 1H), 6.44 (dd, *J* = 8.0 Hz, *J* = 0.8 Hz, 1H), 6.58–6.62 (m, 1H), 6.73 (d, *J* = 7.1 Hz, 2H), 6.77–6.80 (m, 2H), 6.88–6.94 (m, 3H), 6.96–7.03 (m, 3H), 7.04–7.06 (m, 5H), 7.15–7.21 (m, 3H), 7.24–7.29 (m, 2H), 7.53 (q, *J* = 7.7 Hz, 1H), 8.36 (dd, *J* = 8.2 Hz, *J* = 1.3 Hz, 1H), 9.94 (s, 1H), 12.02 (s, 1H). ^{13}C NMR (100 MHz, $CDCl_3$) δ 35.4, 38.0, 56.0, 58.0, 63.7, 66.5, 68.8, 73.1, 111.1, 116.6, 118.6, 120.4, 120.9, 121.1, 122.0, 124.2, 124.7, 125.8, 126.0, 126.3, 127.6, 127.7, 127.8, 128.1, 128.3, 128.9, 129.4, 129.5, 131.6, 134.7, 136.9, 137.7, 138.5, 155.7, 155.8, 155.9, 159.3, 170.2. IR (KBr) 3264, 1682, 1649, 1518, 1449, 751, 703. HRMS(ES^+): calcd for $C_{45}H_{42}N_5O_4$ $(M+H)^+$ 716.3237, found 716.3230.

4.4. Determination of the stoichiometry by ^{1}H NMR titrations (Job plots)

At first, CSA **1** or **2**, (*R*)-**21** and (*S*)-**21** were separately dissolved in $CDCl_3$ with a concentration of 10 mM. These solutions were distributed among nine NMR tubes, with the molar fractions *X* of the guest in the resulting solutions increasing from 0.1 to 0.9, with the total concentration of the host and guest being 10 mM. The ^{1}H NMR spectra of all samples were recorded on a 400 HMz spectrometer. The recorded Job plots of CSA **1**, and (*R*)-**21** and (*S*)-**21** were found to exhibit a maximum at 0.67. This indicates that the CSA **1** forms a 1:2 complex with **21**. However, the recorded Job plots of CSA **2**, and (*R*)-**21** and (*S*)-**21** were found to exhibit a maximum at 0.6. This indicates that CSA **1** forms a 1:1.5 complex with **21**.

4.5. Discrimination ability of CSAs 1 and 2 toward racemic guests 8–24

At first, CSA **1** or **2**, and the guests were separately dissolved in $CDCl_3$ with a concentration of 20 mM. Then, 0.25 mL of CSA **1** or **2** and 0.25 mL guest were added to NMR tubes, so that the total volume was 0.5 mL, and the concentration of CSA and guest was 10 mM. For some less soluble guests, such as **11–14**, **20**, **23**, and **24**, a $CDCl_3/CD_3OD$-5% solution was used as a solvent. In addition, 1 equiv of CSA and 1 equiv of guest **23** were mixed, to which the mixture of $CDCl/CD_3OD$-5%, was added, and the concentration was adjusted to 2.5 mM. The ^{1}H NMR spectra of all samples were recorded on a 400 MHz spectrometer.

4.6. Determination of the enantiomeric purity of guest 21

In order to demonstrate the accuracy of our method for the determination of the enantiomeric excess of the guests, we prepared seven samples containing guest (*R*)-**21** with 60%, 40%, 20%, 0%, −20%, −40%, and −60% ee. All samples were prepared by adding 0.5 equiv of CSA **1** or 1 equiv of CSA **2** into the above solutions with a concentration of 10 mM in $CDCl_3$, and their enantiomeric compositions were determined by using the ^{1}H NMR method on a 400 MHz spectrometer. The results, which were calculated based on the integration of the signals of the CH_3– protons of **21**, are shown in Figures 9 and 10.

Acknowledgement

This work was supported by the Beijing Municipal Commission of Education.

References

1. (a) Bladon, C. *Pharmaceutical Chemistry: Therapeutic Aspects of Biomacromolecules*; Wiley: Chichester, England, 2002; (b) Patric, G. L. *An Introduction to Medicinal Chemistry*; Oxford University Press: New York, 2005; (c) Reetz, M. T. *Angew. Chem., Int. Ed.* **2002**, *41*, 1335–1338; (d) Machida, Y.; Kagawa, M.; Nishi, H. *J. Pharm. Biomed. Anal.* **2003**, *30*, 1929–1942; (e) Ema, T.; Tanida, D.; Hamada, K.; Sakai, T. *J. Org. Chem.* **2008**, *73*, 9129–9132; (f) Naziroglu, H. N.; Durmaz, M.; Bozkurt, S.; Sirit, A. *Chirality* **2011**, *23*, 463–471.
2. (a) Parker, D. *Chem. Res.* **1991**, *91*, 1441–1457; (b) Wenzel, T. J. *Discrimination of Chiral Compounds Using NMR Spectroscopy*; Wiley: Hoboken, NJ, 2007.
3. (a) Kurganov, A. *J. Chromatogr., A* **2001**, *906*, 51–71; (b) Chankvetadze, B.; Blaschke, G. *J. Chromatogr., A* **2001**, *906*, 309–363; (c) Ema, T.; Hamada, K.; Sugita, K.; Nagata, Y.; Sakai, T.; Ohnishi, A. *J. Org. Chem.* **2010**, *75*, 4492–4500.
4. (a) Moon, L. S.; Pal, M.; Kasetti, Y.; Bharatam, P. V.; Jolly, R. S. *J. Org. Chem.* **2010**, *75*, 5487–5498; (b) Evans, M. A.; Morken, J. P. *J. Am. Chem. Soc.* **2002**, *124*, 9020–9021; (c) Lei, X. X.; Liu, L.; Chen, X. J.; Yu, X. C.; Ding, L. S.; Zhang, A. J. *Org. Lett.* **2010**, *12*, 2540–2543.
5. (a) Du, C. P.; You, J. S.; Yu, X. Q.; Liu, C. L.; Lan, J. B.; Xie, R. G. *Tetrahedron: Asymmetry* **2003**, *14*, 3651–3656; (b) Tsubaki, K.; Tanima, D.; Nuruzzaman, M.; Kusumoto, T.; Fuji, K.; Kawabata, T. *J. Org. Chem.* **2005**, *70*, 4609–4616; (c) Demirtas, H. N.; Bozkurt, S.; Durmaz, M.; Yilmaz, M.; Sirit, A. *Tetrahedron* **2009**, *65*, 3014–3018.
6. (a) Li, Z. B.; Lin, J.; Pu, L. *Angew. Chem., Int. Ed.* **2005**, *44*, 1690–1693; (b) Qing, G. Y.; He, Y. B.; Wang, F.; Qin, H. J.; Hu, C. G.; Yang, X. *Eur. J. Org. Chem.* **2007**, 1768–1778; (c) Alfonso, I.; Burguete, M. I.; Galindo, F.; Luis, S. V.; Vigara, L. *J. Org. Chem.* **2009**, *74*, 6130–6142; (d) Liu, H. L.; Peng, Q.; Wu, Y. D.; Chen, D.; Hou, X. L.; Sabat, M.; Pu, L. *Angew. Chem., Int. Ed.* **2010**, *49*, 602–606.
7. (a) Weisman, G. R. In *Asymmetric Synthesis*; Morrison, J. D., Ed.; Academic Press: New York, 1983; Vol. 1, (b) Fraser, R. R. In *Asymmetric Synthesis*; Morrison, J. D., Ed.; Academic Press: New YORK, 1983; Vol. 1, (c) Wenzel, T. J.; Wilcox, J. D. *Chirality* **2003**, *15*, 256–270; (d) Seco, J. M.; Quiñoá, E.; Riguera, R. *Chem. Rev.* **2004**, *104*, 17–117; (e) Sunkur, M.; Baris, D.; Hosgoren, H.; Togrul, M. *J. Org. Chem.* **2008**, *73*, 2570–2575; (f) Quinn, T. P.; Atwood, P. D.; Tanski, J. M.; Moore, T. F.; Folmer-Anderson, J. F. *J. Org. Chem.* **2011**, *76*, 10020–10030.
8. (a) Inamoto, A.; Ogasawara, K.; Omata, K.; Kabuto, K.; Sasaki, Y. *Org. Lett.* **2000**, *2*, 3543–3545; (b) Wenzel, T. J.; Freeman, B. E.; Sek, D. C.; Zopf, J. J.; Nakamura, T.; Yongzhu, J.; Hirose, K.; Tobe, Y. *Anal. Bioanal. Chem.* **2004**, *378*, 1536–1547.
9. Wenzel, T. J.; Amonoo, E. P.; Shariff, S. S.; Aniagyei, S. E. *Tetrahedron: Asymmetry* **2003**, *14*, 3099–3104.
10. (a) Wenzel, T. J.; Thurston, J. E. *J. Org. Chem.* **2000**, *65*, 1243–1248; (b) Wenzel, T. J.; Thurston, J. E.; Sek, D. C.; Joly, J.-P. *Tetrahedron: Asymmetry* **2001**, *12*, 1125–1130; (c) Lovely, A. E.; Wenzel, T. J. *J. Org. Chem.* **2006**, *71*, 9178–9182; (d) Wenzel, T. J.; Bourne, C. E.; Clark, R. L. *Tetrahedron: Asymmetry* **2009**, *20*, 2052–2060; (e) Turgut, Y.; Aral, T.; Hosgoren, H. *Tetrahedron: Asymmetry* **2009**, *20*, 2293–2298.
11. (a) Claeys-Bruno, M.; Toronto, D.; Pécaut, J.; Bardet, M.; Marchon, J.-C. *J. Am. Chem. Soc.* **2001**, *123*, 11067–11068; (b) Ema, T.; Ouchi, N.; Doi, T.; Korenaga, T.; Sakai, T. *Org. Lett.* **2005**, *7*, 3985–3988.
12. (a) Ito, K.; Noike, M.; Kida, A.; Ohba, Y. *J. Org. Chem.* **2002**, *67*, 7519–7522; (b) Zheng, Y. S.; Zhang, C. *Org. Lett.* **2004**, *6*, 1189–1192; (c) Narumi, F.; Hattori, T.; Matsumura, N.; Onodera, T.; Katagiri, H.; Kabuto, C.; Kameyama, H.; Miyano, S. *Tetrahedron* **2004**, *60*, 7827–7833.
13. (a) Yang, D.; Li, X.; Fan, Y.-F.; Zhang, D.-W. *J. Am. Chem. Soc.* **2005**, *127*, 7996–7997; (b) Cuevas, F.; Ballester, P.; Pericàs, M. A. *Org. Lett.* **2005**, *7*, 5485–5487; (c) Iwaniuk, D. P.; Wolf, C. *J. Org. Chem.* **2010**, *75*, 6724–6727.
14. (a) Altava, B.; Barbosa, D. S.; Burguete, M. I.; Escorihuela, J.; Luis, S. V. *Tetrahedron: Asymmetry* **2009**, *20*, 999–1003; (b) Bozkurt, S.; Durmaz, M.; Naziroglu, H. N.; Yilmaz, M.; Sirit, A. *Tetrahedron: Asymmetry* **2011**, *22*, 541–549; (c) Tripathi, A.; Kumar, A.; Pandey, P. S. *Tetrahedron Lett.* **2012**, *53*, 5745–5748.
15. (a) Zhang, X. X.; Bradshaw, J. S.; Izatt, R. M. *Chem. Rev.* **1997**, *97*, 3313–3361; (b) Ema, T.; Tanida, D.; Sakai, T. *J. Am. Chem. Soc.* **2007**, *129*, 10591–10596; (c) Ma, F. N.; Ai, L.; Shen, X. M.; Zhang, C. *Org. Lett.* **2007**, *9*, 125–127; (d) Ma, F. N.; Shen, X. M.; Ming, X.; Wang, J. M.; Ou-Yang, J.; Zhang, C. *Tetrahedron: Asymmetry* **2008**, *19*, 1576–1586.
16. Dahiya, R. *Pak. J. Pharm. Sci.* **2007**, *20*, 317–323.
17. Curini, M.; Epifano, F.; Maltese, F.; Marcotullio, M. C. *Tetrahedron Lett.* **2002**, *43*, 3821–3823.
18. (a) Shono, T.; Kise, N.; Oike, H.; Yoshimoto, M.; Okazaki, E. *Tetrahedron Lett.* **1992**, *33*, 5559–5562; (b) Kise, N.; Okie, H.; Okazaki, E.; Yoshimoto, M.; Shono, T. *J. Org. Chem.* **1995**, *60*, 3980–3992; (c) Kise, N.; Iwasaki, T.; Yasuda, Y.; Sakurai, T. *Tetrahedron Lett.* **2008**, *49*, 7074–7077.
19. Crystal data for $2{\cdot}\mathbf{2}{\cdot}CH_3COCH_3{\cdot}2{\cdot}CH_3OH$: $C_{95}H_{96}N_{10}O_{11}$; M = 1553.82; colorless, triclinic, space group $P1$; a = 9.4373(7) Å, b = 12.8563(10) Å, c = 17.2237(13) Å; V = 2022.8(3) Å^3; μ = 0.084 mm^{-1}; Z = 1; T = 110(2) K; F_{000} = 824; R_1 = 0.0403, wR_2 = 0.0987. The crystallographic data have been deposited at the Cambridge Crystallographic Data Center (CCDC) under deposition number 890101.
20. Frisch, M. J.; Trucks, G. W.; Schlegel, H. B.; Scuseria, G. E.; Robb, M. A.; Cheeseman, J. R.; Montgomery, J. A.; Vreven, T., Jr.; Kudin, K. N.; Burant, J. C.; Millam, J. M.; Iyengar, S. S.; Tomasi, J.; Barone, V.; Mennucci, B.; Cossi, M.; Scalmani, G.; Rega, N.; Petersson, G. A.; Nakatsuji, H.; Hada, M.; Ehara, M.; Toyota, K.; Fukuda, R.; Hasegawa, J.; Ishida, M.; Nakajima, T.; Honda, Y.; Kitao, O.; Nakai, H.; Klene, M.; Li, X.; Knox, J. E.; Hratchian, H. P.; Cross, J. B.; Bakken, V.; Adamo, C.; Jaramillo, J.; Gomperts, R.; Stratmann, R. E.; Yazyev, O.; Austin, A.

J.; Cammi, R.; Pomelli, C.; Ochterski, J. W.; Ayala, P. Y.; Morokuma, K.; Voth, G. A.; Salvador, P.; Dannenberg, J. J.; Zakrzewski, V. G.; Dapprich, S.; Daniels, A. D.; Strain, M. C.; Farkas, O.; Malick, D. K.; Rabuck, A. D.; Raghavachari, K.; Foresman, J. B.; Ortiz, J. V.; Cui, Q.; Baboul, A. G.; Clifford, S.; Cioslowski, J.; Stefanov, B. B.; Liu, G.; Liashenko, A.; Piskorz, P.; Komaromi, I.; Martin, R. L.; Fox, D. J.; Keith, T.; Al-Laham, M. A.; Peng, C. Y.; Nanayakkara, A.; Challacombe, M.; Gill, P. M. W.; Johnson, B.; Chen, W.; Wong, M. W.; Gonzalez, C.; Pople, J. A. *GAUSSIAN 03*; Gaussian, Inc.: Wallingford CT, 2004.